Cure Kinetics of a Flexible Aromatic Dicyanate with Schiff Base Structure

YING-HUNG WANG, YENG-LONG HONG, and JIN-LONG HONG*

Department of Chemistry and Institute of Materials Science and Engineering, National Sun Yat-Sen University, Kaohsiung, Taiwan 80424, Republic of China

SYNOPSIS

Polycyclotrimerization of a flexible aromatic dicyanate with a Schiff base structure was studied by means of differential scanning calorimetry (DSC). The study on dynamic DSC evaluated an apparent activation energy (E_a) of 75.8 kJ/mol and autocatalytic *first*-order kinetics with rate expression $Af(\alpha) = 1.96 \times 10^5 (1 + 4.39\ \alpha)(1 - \alpha)\ \text{min}^{-1}$. The kinetic feature can be explained by a proposed mechanism consisting of hydroxyl-catalyzed and autocatalytic paths. The lower value of E_a compared with other aromatic dicyanates is due to the electron-withdrawing linkage of the inherent imine (—CH=N) structure. The kinetic feature is affected by the content of the residual impurities (e.g., phenols or absorbed water) in the corresponding sample. © 1995 John Wiley & Sons, Inc.

INTRODUCTION

Cyclotrimerization of cyanates is an interesting reaction since it involves the formation of a *sym*-triazine ring from three cyanate groups as shown in Figure 1. The extension of cyclotrimerization to aromatic dicyanates leads to the construction of a polymeric network with *sym*-triazine crosslinks. This reaction, referred to as polycyclotrimerization, may be catalyzed by transition-metal carboxylates or acetylacetonates[1-5] or by phenols.[4-6] In the absence of externally added catalysts, the polycyclotrimerization reaction is believed to be catalyzed by the residual hydrogen-donating impurities such as phenol substances and water.[6] No reaction takes place if pure aromatic dicyanates are heated. The detailed kinetics of the polycyclotrimerization reaction, however, appears rather complicated as observed from previous kinetic studies.

Using Cr^{3+} acetylacetonate [$Cr(acac)_3$] as a catalyst, Bonetskaya et al.[1,5,7] studied the polycyclotrimerization of bisphenol A dicyanate (BPADCy) in ditolylmethane using infrared spectroscopy (IR). They observed that there existed a maximum rate (i.e., the reaction bears autocatalytic characteristics) at a definite degree of conversion independent of the initial monomer concentration or the catalyst concentration. This maximum rate itself was proportional to the square-root of the catalyst and water concentration and depends linearly on the monomer concentration. An autocatalytic *first*-order kinetic was constructed based on a coordination/ionic reaction mechanism. For comparison, Bauer et al.[6,8] studied the cure of BPADCy with IR. Without the presence of any catalyst (but with 0.5–1.5% of phenol residues as they claimed), a *first*-order rate expression resulted. Also, a reaction mechanism without any autocatalytic step was proposed.

Results of the two pioneering groups, however, were not confirmed by other workers. Cure kinetics of a commercialized aromatic dicyanate (as PBMBDCy in Table I) was studied by Simon et al.[3,9,10] For the uncatalyzed resin (i.e., without the presence of externally added catalyst), the rate of reaction was slow and could be fitted with an empirical rate expression of

$$d\alpha/dt = (k_1 + k_2\ \alpha)(1 - \alpha)^2 \qquad (1)$$

where α is the fractional conversion and k_1 and k_2 are apparent rate constants. The second term on the right-hand side of eq. (1) was due to the con-

* To whom correspondence should be addressed.

Journal of Applied Polymer Science, Vol. 58, 1585–1592 (1995)
© 1995 John Wiley & Sons, Inc. CCC 0021-8995/95/091585-08

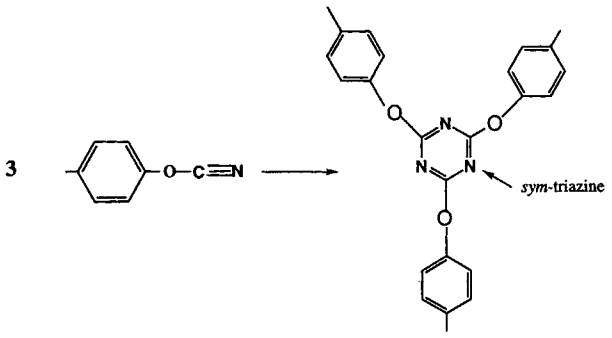

Figure 1 Cyclotrimerization of cyanate groups.

sideration of a competing (and presumably autocatalytic) reaction observed in dynamic DSC thermograms as a second exothermic peak. The corresponding activation energies for k_1 and k_2 were 44 and 134 kJ/mol, respectively. In the presence of a mixture of copper naphthenate and *n*-nonylphenol, the rate of polycyclotrimerization was fitted with a simple *n*th-order expression where an optimal value of $n = 1.872$ was found.[2] The cure behavior of BPADCy in the presence of a mixed catalyst was examined by Osei-Owusu et al.[4,11] An empirical *second*-order rate expression was established. The rate constant was found to depend linearly on the catalyst concentration.

Results from previous kinetic studies can be summarized in Table I,[1,2,4–15] which suggests that they do not agree with one another. One apparent reason for this confusion is the difference in the (often complicated) catalyst systems used by different research groups. It is believed that reaction paths of the organometallic catalysts and the phenolic catalysts (impurity or externally added) can be entirely different: The former proceeds via a coordination/ionic mechanism, whereas the latter, via a nonionic, step-growth route. In addition, most of the aromatic dicyanates used previously were commercial products, which contain certain phenolic residues or water and obscure the kinetic results.

A literature survey indicates that most of the aromatic dicyanates previously used have a rigid structure of two cyanatophenyl units linked by a central carbon or heteroatoms.[15,16] Here, we proposed to study the cure behavior of a flexible aromatic dicyanate of a Schiff-base type (DC in Fig. 2). Dicyanate DC, with its long-chain and flexible aliphatic center, should have different kinetic fea-

Table I Kinetic Rate Equations for Different Aromatic Dicyanates

Authors/Reference[a]	Monomer[b] (Condition)	Catalyst	Instrument	Rate Equation
Bonetakaya et al.[1,5]	BPADCy (solution)	Cr (acac)$_3$ + H_2O	IR	$k\,[C_0]^{0.5}\,(B + \alpha)(1 - \alpha)$
Bauer et al.[6,8]	BPADCy (bulk)	Phenol (0.5–1.5%)	IR, DSC	$k(1 - \alpha)$
Shimp[2]	BPADCy (bulk)	Cu naphthenate + n-nonylphenol	—	—
Simon et al.[9,10]	PBMBDCy (bulk)	Phenol + H_2O	IR	$(k_1 + k_2\,\alpha)(1 - \alpha)^2$
Georjon et al.[12]	BPADCy (bulk)	Phenol + H_2O	IR	$(k_1 + k_2\,\alpha)(1 - \alpha)^2$
Osei-Owusu et al.[4,11]	BPADCy (bulk)	Various	IR	$k[M_0]\,(1 - \alpha)^2$
Zeng et al.[13]	Rex 373 Rex 378	Residual impurities	DSC	$(k_1 + k_2\,\alpha)(1 - \alpha)$
Simon and Gillham[14]	PBMBDCy	Cu naphthenate + n-nonylphenol	IR	$k_1\,(1 - \alpha)^2\alpha + k_2\,(1 - \alpha)^2$
Lin et al.[15]	DTC	Residual impurities	DSC	$k(1 + D\alpha)(1 - \alpha)$

[a] References are indicated by the superscript following the authors' names.

[b]

BADCy:

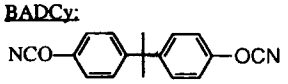

M-30:

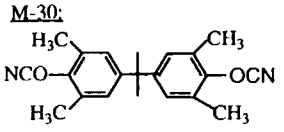

PBMBDCy (REX 378):

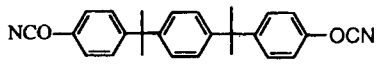

DTC:

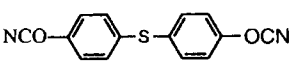

REX 373: 55 % BPADCy
45 % M-30

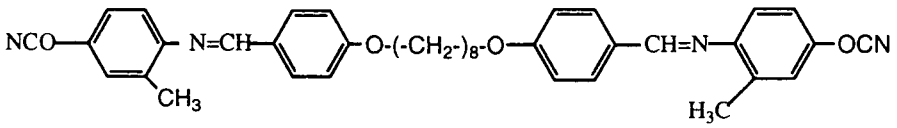

Figure 2 Chemical structure of flexible Schiff base, DC.

tures from the reported cases. Also, DC, as prepared and purified via vigorous condition, may reduce the uncertainty of the kinetic result due to the presence of minor impurities.

EXPERIMENTAL

Flexible Schiff base DC (structure shown in Fig. 2) was prepared according to the brief procedures described previously.[17] A crude product of DC was washed with acetone twice and the residual solid was recrystallized from methylene chloride/hexane to give a final product. The sample was examined by a 300 MHz ^{1}H-NMR to detect any residual phenolic OH peak from δ 8.0–10.0. The sample was mixed with KBr powder and pressed to make a pellet for IR study. The sample in a Pyrex holder was sitting in a Pyrex gas cell (diameter = 25 mm, length = 150 mm) connected to thermocouples for temperature control. The study was performed at different temperatures under a nitrogen atmosphere. A DuPont DSC 910 cell connected to a DuPont 9900 data station was used for the kinetic study. A sample of approximately 10 mg in weight was sealed in a hermetic aluminum pan and scanned in the calorimeter with a heating rate of 5, 10, 20, or 30°C/min in the temperature range of 50–350°C. The carrier gas was nitrogen at a flow rate of ca. 10 mL/min. Calibration of the calorimeter was conducted for each heating rate using an indium standard. For the isothermal study, the DSC cell was heated to the desired temperature and we waited for the system to reach the equilibrium state before loading the sample. Two isothermal temperatures of 200 and 220°C were used in this study.

RESULTS

Polycyclotrimerization of the DC sample can be easily detected by infrared spectroscopy (IR). Figure 3 shows the corresponding IR spectra of DC at 124°C. The cyanate absorption around 2250 cm^{-1} gradually decreased and became a tiny peak after being heated at 124°C for 70 min. The formation of a *sym*-triazine ring can be easily demonstrated by the progressive appearance of absorptions at 1380

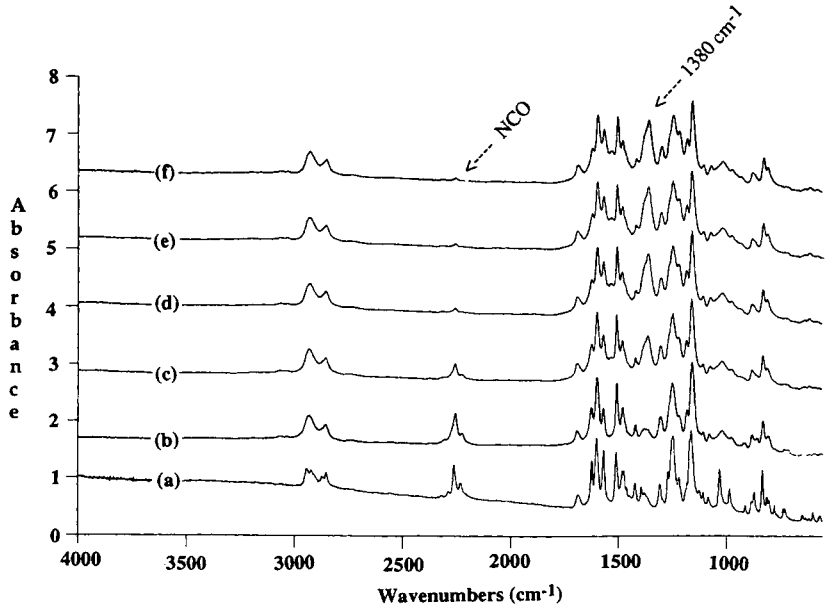

Figure 3 Infrared spectra of DC at (a) room temperature and after heating at 104°C for (b) 1 min, (c) 5 min, (d) 10 min, (e) 15 min.

cm^{-1}). The other *sym*-triazine stretching absorption at 1570 cm^{-1} is overlapped with an imine stretch and cannot be resolved well in this case. Further heating of DC to 200°C resulted in the disappearance of a cyanate peak at around 2250 cm^{-1}, indicating the completeness of the polycyclotrimerization.

Sample DC was subjected to a kinetic study with differential scanning calorimetry (DSC). The DSC thermograms given in Figure 4 show a melting endotherm followed by a cure exotherm, representing the progression of polycyclotrimerization. By analyzing the curing exotherm, cure kinetics can be evaluated. Primarily, we may consider that any reaction rate can be expressed with a simple form of

$$d\alpha/dt = kf(\alpha) = Af(\alpha)\exp(-E_a/RT) \quad (2)$$

where $f(\alpha)$ represents the concentration-dependent part of the rate expression; $k = A\exp(-E_a/RT)$ is the rate constant; A is the preexponential factor; E_a, the apparent activation energy; R, the gas constant, and T, the absolute temperature. It has been observed that the extent of the reaction at the peak temperature (T_p, temperature at maximum rate of reaction) is constant and independent of the heating rate for many thermosetting systems.[18–22] Integration of $1/f(\alpha)$ from $\alpha = 0$ to α_p (peak conversion; the corresponding conversion at T_p) should yield a constant value and the following relationship was therefore deduced by Prime:[18]

$$E_a = -0.951R[d\ln\Phi/d(1/T_p)] \quad (3)$$

where Φ is the heating rate. Table II summarizes the data adapted from the dynamic DSC runs. The peak conversion (α_p) is nearly independent of the heating rate. The plot of $\ln\Phi$ vs. the reciprocal peak temperature is given in Figure 5. The apparent activation energy thus obtained is 75.8 kJ/mol, a value comparatively less than the published one of 92.6 kJ/mol for polycyclotrimerization of 4,4′-thiodiphenylcyanate.

Further manipulation of eq. (2) can be performed by taking the E_a value and the experimental $d\alpha/dt$ data to obtain $Af(\alpha)$ by

$$Af(\alpha) = [d\alpha/dt]\exp(E_a/RT) \quad (4)$$

For a simple nth-order reaction, the relationship $\ln[Af(\alpha)] = \ln A + n\ln(1-\alpha)$ should hold; however, the resulting $\ln[Af(\alpha)]$ and $\ln(1-\alpha)$ are not linearly related. Further fitting of $\ln[Af(\alpha)]/(1-\alpha)$ vs. α resulted in a linear curve (Fig. 6). Therefore, the autocatalytic *first*-order rate expression of

$$Af(\alpha) = 1.96\times10^5(1+4.39\alpha)\times(1-\alpha)\ \text{min}^{-1} \quad (5)$$

can be used to represent the cure of DC. Further treatment would require the incorporation of the E_a value into eq. (5); thus, a direct rate expression can be obtained in the form of eq. (2). Temperature integration can be achieved by the application of dT/dt ($= \Phi$) into eq. (2) and this resulted in a conversion–time curve. The calculated curves are cor-

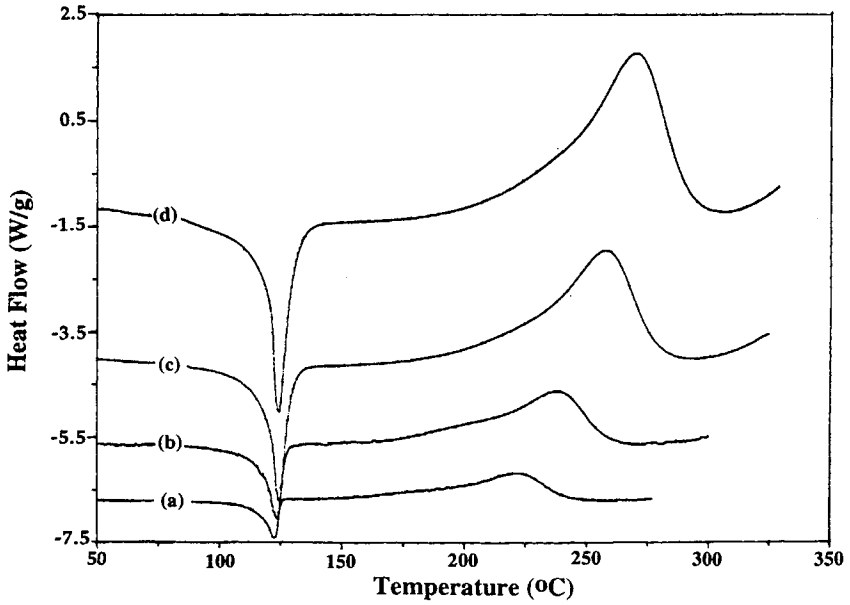

Figure 4 DSC thermograms of DC at various heating rates (Φ). Curve (a) Φ = 5°C/min, (b) Φ = 10°C/min, (c) Φ = 20°C/min, (d) Φ = 30°C/min.

Table II Peak Conversion (α_p) and Peak Temperature (T_p) at Different Heating Rates

Heating Rate (°C/min)	Peak Conversion (α_p, %)	Peak Temperature (T_p, °C)
5	68.3	221
10	69.5	238
20	68.7	258
30	68.6	271

related well with the experimental results as shown in Figure 7. Moreover, eq. (5) can be used to compare with the isothermal results. Traces of isothermal DSC scans at 200 and 220°C are given in Figure 8 and the reaction rate ($d\alpha/dt$) can be directly adapted from these thermograms. Figure 9 demonstrates that the kinetic expression of eq. (5) from dynamic runs can also be used to illustrate the isothermal cure.

DISCUSSION

The mechanism for cyclotrimerization of aromatic dicyanate previously proposed by Bauer et al.[6] suggested the necessity of an impure hydroxyl group as a catalyst to initialize the reaction. This mechanism recommended the principal pathways of cyclotrimerization, but cannot explain the autocatalyzed nature observed from this study. Therefore, a mechanistic pathway, consisting of hydroxyl-catalyzed and autocatalyzed reactions, in Scheme 1 was proposed. Reaction steps in the hydroxyl-catalyzed part are basically similar to Bauer et al.'s proposal, while steps in the autocatalyzed part ran in a parallel manner with those in hydroxyl-catalyzed counterpart except that all species (such as HM_3, X_1^*, and

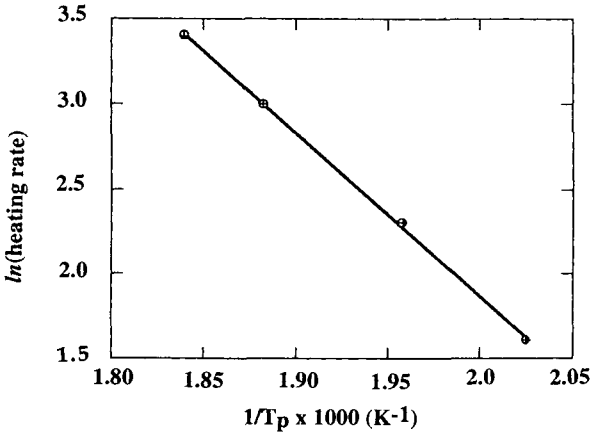

Figure 5 Linear relationship between *ln*(heating rate) and reciprocal peak temperature ($1/T_p$).

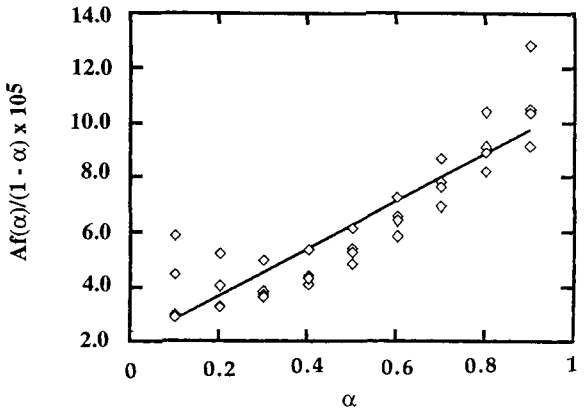

Figure 6 Plot of $Af(\alpha)/(1-\alpha)$ vs. α for DC. Symbols represent data from dynamic DSC scans. The solid line is the least-square fit.

X_2^*) involved are coordinated to the *sym*-triazine ring through hydrogen bonding. Under the assumptions of a pseudo-steady state and that steps 1 and 6 are the rate-determining steps ($d[S^*]/dt = 0$, where S^* denotes the involved species such as M_1^*, M_2^*, M_3^*, HM_3, X_1^*, and X_2^*), a routine kinetic analysis on this mechanistic scheme may result in a kinetic expression of

$$-[d[M]/dt = [BH][M](k_1 + (k_5/k_{-5})k_6[M_3]) \quad (6)$$

where k_i (or k_{-i}) is the rate constant of the respective forward (or backward) reaction of step i, and [M], [BH], and [M_3] represent the concentrations of monomer, active-hydrogen species, and *sym*-triazine, respectively. This autocatalytic *first*-order

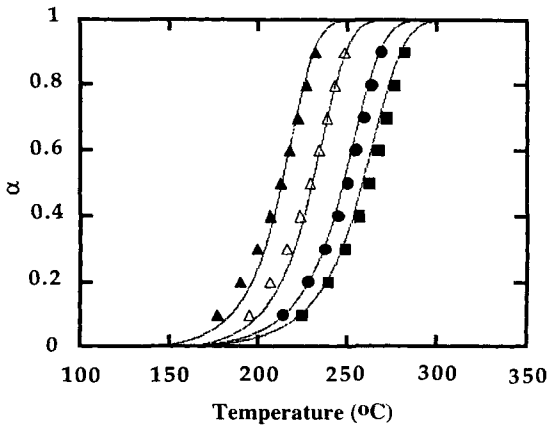

Figure 7 Comparison between experimentally determined conversion curves (symbols) and those (solid lines) calculated from the empirical rate expression. The corresponding heating rates of the conversion curves are, from left to right, 5, 10, 20, and 30°C/min, respectively.

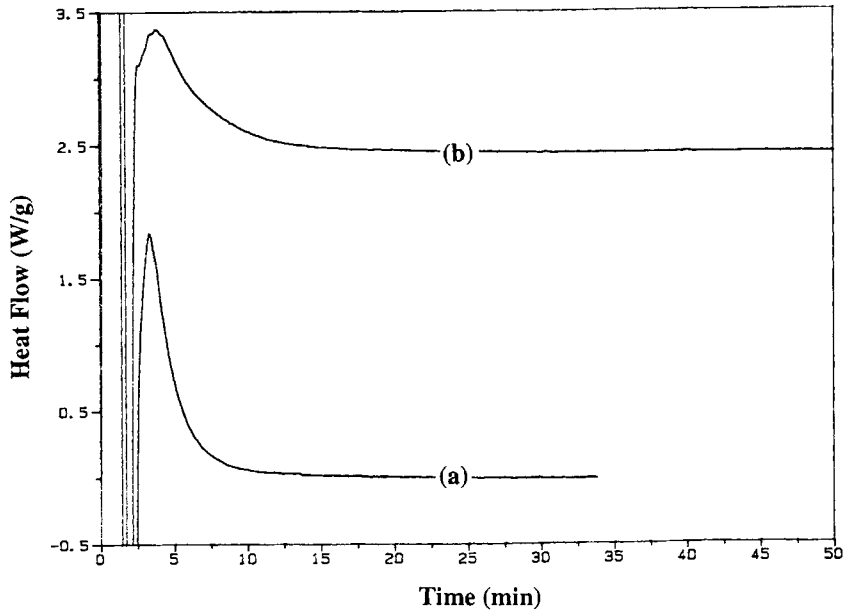

Figure 8 DSC thermograms of DC sample heated at (a) 220 and (b) 200.

rate is in good agreement with our experimental findings.

Basically, step 1 (or 6) involve the nucleophilic addition of active hydrogen species, BH (or the coordinated BH species, HM_3), to cyanate. As mentioned above, BH may be water or the phenol substances, whose quantities in the sample is presumably low. Therefore, steps 1 and 6 as rate-determining steps is a reasonable assumption. In samples containing larger amounts of active hydrogen species, nucleophilic addition of BH (or HM_3) to cyanate involved in steps 1 and 6 may not be so difficult; instead, steps 2 and 7 become the rate-determining steps. Similar deduction procedures based on steps 2 and 7 as rate-determining steps resulted in an autocatalytic *second*-order kinetics.

The autocatalytic function of the *s*-triazine ring required further comment. Generally, we observed that a partially cured sample has lower curing temperatures than does the uncured one. For example, a 43%-cured DC sample has a curing exotherm with its on-set temperature at 80°C and peak temperature at 164°C (heating rate = 20°C/min), obviously lower than those of the uncured sample [compared with curve (*c*) in Fig. 4]. Presumably, the *s*-triazine formed in this partially cured sample serves as a catalyst for cyclotrimerization. A similar phenomenon was observed in our study for 4,4′-thiodiphenylcyante (TDC, NCO–Ph–S–Ph–OCN).[23] As mentioned above, the resulting *first*-order kinetics basically concerned the amounts of phenols or water impurities, which are difficult to assess. Nevertheless, our previous results on TDC may provide certain clues for us to judge the impurities' level. Different amounts (1–10 phr) of *n*-nonylphenol were added to TDC and the kinetics features of the resulting mixture were studied by the same method applied in this research. The data can be fitted into a *second*-order autocatalytic rate expression with its autocatalytic contribution remaining constant but the preexponential factor, related to the amounts of *n*-nonylphenol. The resulting data for the DC sam-

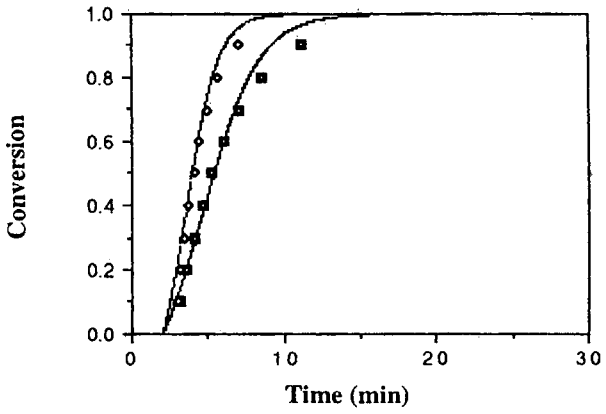

Figure 9 Comparison between experimentally determined conversion curves (symbols) and those (solid lines) calculated from the empirical rate expression. The corresponding DSC traces are, from left to right, adapted from isothermal heatings at 200 and 220°C, respectively.

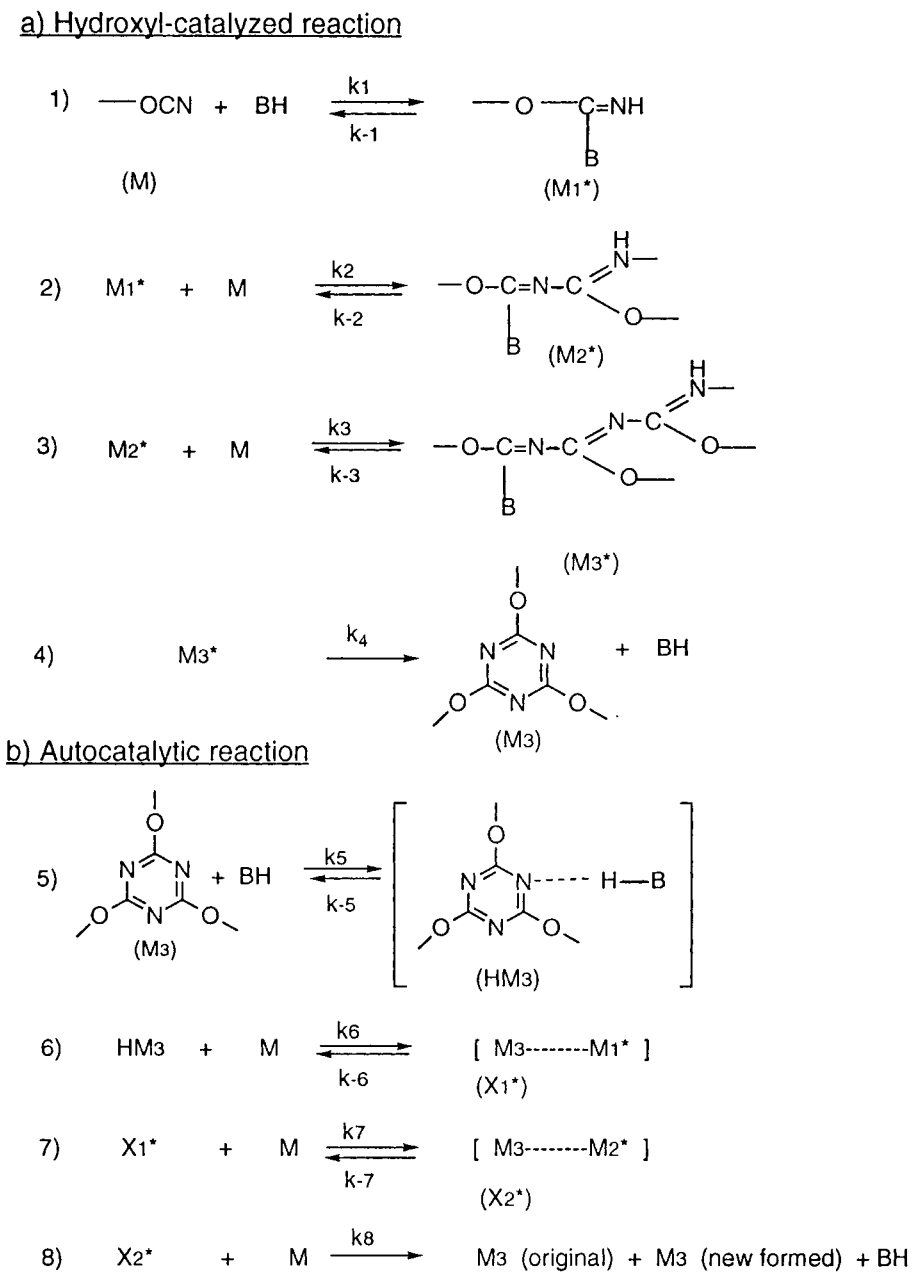

Scheme 1 Proposed mechanistic pathways of polycyclotrimerization.

ple cannot be fitted well with *second*-order autocatalytic kinetics, which may suggest that its impurities' level of phenols is low. To further evaluate the effect of water, the TDC sample was exposed to moisture and its DSC thermograms compared with the unexposed one. The result suggests that moisture can drastically lower its curing exotherm from an onset of 200–120°C and peak temperature of 320–280°C. Also, the exothermic peak became broader and less symmetical in shape. The curing temperatures of the DC sample were resonably high, indicating that its moisture content is low.

The parameters evaluated in this study can also be further compared with the results from TDC.[15] The cure of TDC has an apparent activation energy (E_a) of 92.6 kJ/mol, higher than that of DC. This may be due to the difference between the chemical structures of TDC and DC. As suggested by the mechanistic steps listed in Scheme 1, E_a should be affected by the electrophilicity of the cyanate groups.

Cyanate with electron-withdrawing linkage (i.e., —N=CH— in DC) would be easier to be attacked by nucleophiles than that with electron-donating linkage (i.e., —S— in TDC).

CONCLUSION

An autocatalytic *first*-order rate expression, $d\alpha/dt = 1.96 \times 10^5 (1 + 4.39\alpha)(1 - \alpha)\ \text{min}^{-1}$, can be used to illustrate the cure behavior of the flexible Schiff base, DC. The kinetic result was explained by the mechanistic steps listed in Scheme 1. The kinetic feature is affected by the content of the residual impurities (e.g., phenols or absorbed water). The low apparent activation energy (E_a) is explained by the inherent electron-withdrawing CH=N linkage, which reduces E_a due to the increasing feasibility of the nucleophilic addition of BH to cyanate.

This work was financially supported by the National Science Council, R.O.C., under Contract Number NSC83-0405-E110-012.

REFERENCES

1. A. K. Bonetskaya, V. V. Ivanov, M. A. Kravchenko, V. A. Pankratov, Ts. M. Frenkel, V. V. Korshak, and S. V. Vinogradova, *Polym. Sci. U.S.S.R.*, **22,** 845 (1980).
2. D. A. Shimp, *Polym. Mater. Sci. Eng.*, **54,** 107 (1986).
3. S. L. Simon, J. K. Gillham, and D. A. Shimp, *Polym. Mater. Sci. Eng.*, **62,** 96 (1990).
4. A. Osei-Owusu and G. C. Martin, *Polym. Mater. Sci. Eng.*, **65,** 304 (1991).
5. A. K. Bonetskaya, M. A. Kravchenko, Ts. M. Frenkel, V. A. Pankratov, S. V. Vinogradova, and V. V. Korshak, *Polym. Sci. U.S.S.R.*, **19,** 1201 (1977).
6. M. Bauer, J. Bauer, and G. Kuhn, *Acta Polym.*, **37,** 715 (1986).
7. V. V. Korshak, V. A. Pankratov, A. A. Ladovskaya, and S. V. Vinogradova, *J. Polym. Sci., Polym. Chem. Ed.*, **16,** 1697 (1978).
8. M. Bauer, J. Bauer, and B. Garske, *Acta Polym.*, **37,** 604 (1986).
9. S. L. Simon and J. K. Gillham, *Polym. Prepr. Am. Chem. Soc. Div. Polym. Sci.*, **32,** 182 (1991).
10. S. L. Simon and J. K. Gillham, *J. Appl. Polym. Sci.*, **47,** 461 (1993).
11. A. Osei-Owusu, G. C. Martin, and J. T. Gotro, *Polym. Eng. Sci.*, **32,** 535 (1992).
12. O. Georjon, J. Galy, and J. P. Pascault, *J. Appl. Polym. Sci.*, **49,** 1441 (1993).
13. S. Zeng, K. Ahn, J. C. Seferis, and J. M. Kenny, *Polym. Compos.*, **13,** 191 (1992).
14. S. L. Simon and J. K. Gillham, *Polym. Mater. Sci. Eng.*, **66,** 453 (1992).
15. R. H. Lin, J. L. Hong, and A. C. Su, *Polym. Mater. Sci. Eng.*, **66,** 464 (1992).
16. A. M. Gupta and C. W. Macosko, *Macromolecules,* **26,** 2455 (1993).
17. Y. H. Wang, V. Y. L. Hong, and J. L. Hong, *Polymer,* **34,** 1970 (1993).
18. R. B. Prime, *Polym. Eng. Sci.*, **13,** 365 (1973).
19. N. H. Horowitz and G. Metzger, *Anal. Chem.*, **35,** 1464 (1963).
20. P. Pryser and W. D. Bascom, *Anal. Calorim.*, **3,** 537 (1974).
21. T. H. Hsieh and A. C. Su, *J. Appl. Polym. Sci.*, **41,** 1271 (1990).
22. J. L. Hong, C. K. Wang and R. H. Lin, *J. Appl. Polym. Sci.*, **53,** 105 (1994).
23. R. H. Lin, J. L. Hong, and A. C. Su, *Polymer,* to appear.

Received March 1, 1995
Accepted May 5, 1995